NANO-MICRO LETTERS ARTICLE
www.nmletters.org

Hydrothermal Synthesis and Characterization of Europium-doped Barium Titanate Nanocrystallites

Margarita García-Hernández[1,*], Geneviève Chadeyron[2], Damien Boyer[2], Antonieta García-Murillo[3], Felipe Carrillo-Romo[3], Rachid Mahiou[2]

(Received 19 February 2013; accepted 18 March 2013; published online 25 March 2013)

Abstract: Barium titanate nanocrystallites were synthesized by a hydrothermal technique from barium chloride and tetrabutyl titanate. Single-crystalline cubic perovskite $BaTiO_3$ consisting of spherical particles with diameters ranging from 10 to 30 nm was easily achieved by this route. In order to study the influence of the synthesis process on the morphology and the optical properties, barium titanate was also prepared by a solid-state reaction. In this case, only the tetragonal phase which crystallizes above 900°C was observed. High-temperature X-ray diffraction measurements were performed to investigate the crystallization temperatures as well as the particle sizes via the Scherrer formula. The lattice vibrations were evidenced by infrared spectroscopy. Eu^{3+} was used as a structural probe, and the luminescence properties recorded from $BaTiO_3$:$Eu^{3+}$and elaborated by a solid-state reaction and hydrothermal process were compared. The reddish emission of the europium is increased by the nanometric particles.
Keywords: $BaTiO_3$; Europium; Nanocrystallites; Hydrothermal technique

Citation: Margarita García-Hernández, Geneviève Chadeyron, Damien Boyer, Antonieta García-Murillo, Felipe Carrillo-Romo and Rachid Mahiou, "Hydrothermal Synthesis and Characterization of Europium-doped Barium Titanate Nanocrystallites", Nano-Micro Lett. 5(1), 57-65 (2013). http://dx.doi.org/10.3786/nml.v5i1.p57-65

Introduction

$BaTiO_3$ is one of the most widely used ferroelectric materials, especially for the manufacture of thermistors, electro-optics devices and multilayered capacitors (MLCCs) [1,2]. Many researches are devoted to diminishing the size of $BaTiO_3$ crystals in order to fulfill the requirements of nanoelectronic devices. When they are doped with lanthanide ions, insulating materials exhibit optical properties, which are greatly dependent on the crystals' size [3]. As a consequence the studies related on the luminescence properties of newly doped nanostructured systems with rare earth elements have been increased as an efficient tool to investigate the insulating materials' size [4]. In particular, barium titanate has been studied regarding its luminescent properties when doped with rare earth elements such as Eu^{3+} [3], Yb^{3+} [4,5] and Er^{3+} [6]. Its perovskite structure allows hosting ions of a different size, and a high concen-

[1]Universidad Autónoma Metropolitana, Departamento de Ciencias Naturales, DCNI, Unidad Cuajimalpa, Pedro Antonio de los Santos 84, 11850 México D.F. México. Email: mgarciah@correo.cua.uam.mx (M.G.H.).
[2]Clermont Université Institut de Chimie de Clermont-Ferrand, UMR 6296, CNRS/UBP/ENSCCF, BP 10448, F-63000 Clermont-Ferrand. Email: chadeyr@chimie.univ-bpclermont.fr (G.C.), damien.boyer@ensccf.fr (D.B.), Rachid.MAHIOU@univ-bpclermont.fr (R.M.).
[3]Instituto Politécnico Nacional, CIITEC IPN, Cerrada de Cecati S/N. Col. Santa Catarina, Azcapotzalco México D.F. C.P. 02250, México. Email: angarciam@ipn.mx (A.G.M.), fcarrillo@ipn.mx (F.C.R.).
*Corresponding author. E-mail: mgarciah@correo.cua.uam.mx (M.G.H.), Tel.: +52 (55) 2636 38 00 ext. 3857, Fax: +52 (55) 2636 38 00 ext. 3832.

tration of doping ions can be accommodated without major difficulties. Therefore, recently there has been a tremendous interest to prepare such materials.

The conventional solid-state reaction to synthesizing ceramics requires a calcination step at high temperature for enhancing the diffusivity between raw solid materials,whereby resulting in the increase of grain size. To overcome such a drawback, wet chemical routes have been intensively investigated because they allow a better control of the granulometric distribution and lead to highly pure $BaTiO_3$ nanocrystals, e.g. by using a hydrothermal method [7-11], sol-gel process [12-16], oxalate route [17], micro-emulsion process [18], microwave heating [19], polymeric precursor method [20], and homogeneous coprecipitation [21]. The hydrothermal synthesis of ceramic powders is of great interest because of the possibility to prepare pure and ultrafine particles with narrow size distribution from inexpensive and easily accessible precursors in a single step [22]. Hence, the synthesis can be performed at moderate temperature and pressure using a simple autoclave. Varying the chemical process parameters, such as reagent concentrations, temperature, pressure, and pH, can optimize the conditions of a hydrothermal reaction. Several polymorphic varieties of $BaTiO_3$ have already been isolated: rhombohedral, orthorhombic, tetragonal, cubic, and hexagonal [23].

It is well known that the ferroelectricity degree of $BaTiO_3$ decreases when decreasing the particle size, and disappears below a certain critical size because of the crystallographic phase transition from tetragonal to cubic [24]. A limit size of 50 nm has been postulated by Ishikawa et al. [25] and Schlag et al. [26] as being critical for ferroelectric properties of $BaTiO_3$. Few studies have already described the preparation of Eu^{3+}-doped $BaTiO_3$ using the hydrothermal method [27,28]. In the present work, nanocrystallites of $BaTiO_3$:Eu^{3+} (5 mol %) were obtained by an original synthesis procedure using a hydrothermal method (hm). $BaTiO_3$:Eu^{3+} (5 mol%) powders were also synthesized by using the solid-state reaction (ssr) for comparison. The samples were characterized by X-ray diffraction (XRD), differential thermal analysis (DTA), FTIR and Raman spectroscopies as well as scanning and transmission electron microscopies (SEM and TEM). Furthermore, the photoluminescence properties were recorded for both samples.

Experimental Section

Preparation of barium titanate powders by hydrothermal synthesis

Barium titanate was prepared via a hydrothermal route according to the following procedure. All experiments were carried out at room temperature under an inert atmosphere. $BaCl_2$ (0.95 eq) and $EuCl_3$ (0.05 eq) were dissolved in a round flask with the appropriate amount of MeOH under vigorous magnetic stirring for 2 h. Then, metallic potassium (2.05 eq.) was added to the reaction mixture, leading to an exothermic reaction and the precipitation of potassium chloride. After 2 h, 1 eq. of titanium (IV) butoxide was introduced drop by drop, with a milky solution being obtained. Thereafter, the suspension obtained above was transferred into a cylindrical autoclave (Teflon-lined stainless steel) filled at 2/3 of its volume. The autoclave was put inside the oven, and the reaction was performed for 24 h at 200℃. After cooling down to room temperature, the insoluble reaction products were washed several times using a solution of 0.1 M HCl and water for removing the excess ions arising from starting materials. Finally, the resulting $BaTiO_3$:Eu^{3+} powders were oven-dried at 90℃ for 24 h.

Preparation of barium titanate powders by solid-state reaction

The detail of sample preparation has been reported in the literature [17]. $BaTiO_3$ was obtained by firing at high temperature a mixture of $BaCO_3$ and TiO_2 powders. Two steps were involved: ball milling for 2 h at 300 rpm and then a sintering at 1150℃ for 4 h.

Characterization techniques

The structures of $BaTiO_3$: Eu^{3+} (5 mol%) powders were determined by an automated powder diffractometer (Philips Xpert Pro) using Cu-K. α radiation at 40 kV and 30 mA. The powder's High-Temperature X-ray diffraction (HT-XRD) data were collected at 25℃ and every 100℃ during the heating/cooling steps between 100 and 1200℃. After putting the sample on a platinum ribbon and reaching the given temperature at 10℃/min, the diffractometer was held at each temperature for 1 h prior to the data collection, and then XRD data were collected for 50 min over the 2θ range 10-70°. The powders were analyzed by DTA and thermo gravimetry (TG) using a Mettler Toledo TGA/SDTA 851e. The thermal cycle applied to collect DTA and TG data consisted of heating hm- and ssr-derived powders, respectively, from room temperature to 800℃ and 1000℃ at 2℃/min upon a nitrogen atmosphere.

The IR transmittance spectra were recorded from powders heat-treated at 1150℃ for 4 h using an FTIR 2000 Perkin-Elmer in the range of 4000-200 cm^{-1}. The samples were analyzed using the KBr and polyethylene pelleting technique for the ranges of 4000-400 cm^{-1} and 400-200 cm^{-1} respectively. The Raman spectra of powders were recorded using a T64000 Jobin-Yvon confocal micro-Raman Spectrometer with a 514 nm wavelength line green laser excitation source (Coherent model 70C5 Ar^+) operating at 800 mW with approximately 1 cm^{-1}

resolution. SEM images of $BaTiO_3$:Eu^{3+} (5 mol%) powders were obtained using a scanning electron microscope (Zeiss Model Supra-55 VP) equipped with an Everhardt Thornley secondary electron (SE) detector operating at 2.5 kV at high-vacuum mode. Conventional Transmission Electron Microscopy (CTEM) was performed on a Hitachi H-7650 at an acceleration voltage of 120 kV. $BaTiO_3$:Eu^{3+} (5% mol) powders were dispersed in water using an ultrasonic bath, with the solution being directly deposited onto a carbon grid.

The luminescence spectra were recorded with a monochromator Jobin-Yvon HR 1000 spectrometer, using a dye laser (continuum ND62) pumped by a frequency-doubled pulsed YAG:Nd^{3+} laser (continuum surelite I). The dye solution was prepared by mixing Rhodamines 610 and 640. To achieve a resonant pumping in the blue wavelength range, the output of the dye laser was up-shifted to 4155 cm^{-1} by stimulated Raman scattering in a high-pressure gaseous H_2 cell.

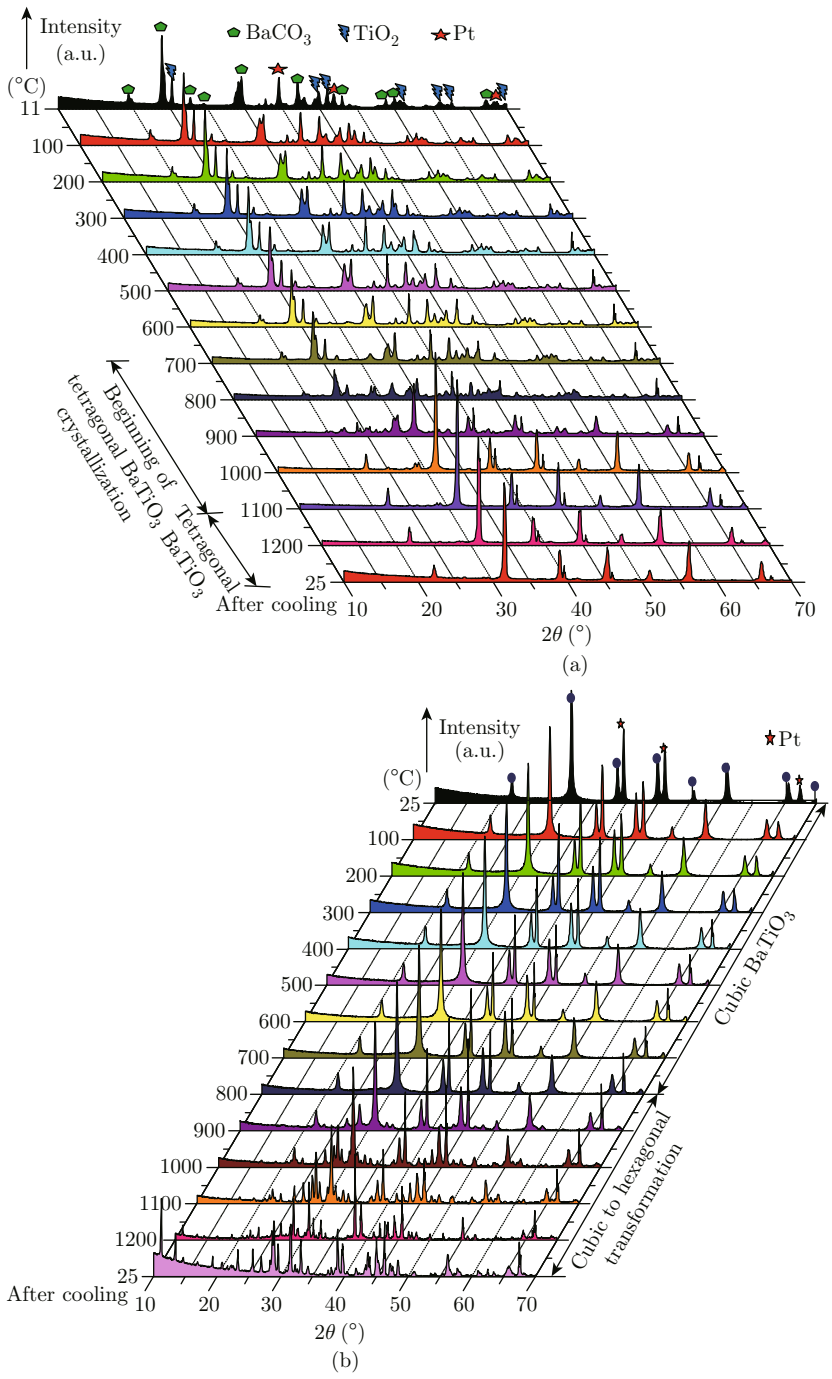

Fig. 1 HTXRD patterns of (a) ssr; (b) hm $BaTiO_3$:Eu^{3+} (5 mol%) powders.

Result and discussion

XRD analysis

To investigate the structural characteristics of the $BaTiO_3$:Eu^{3+} synthesized by a solid-state reaction, the samples were put directly in the HTXRD chamber just after the ball milling without 4h heat treatment at 1150℃. Figure 1(a) shows the HTXRD diffraction patterns. The first scan corresponds to the pattern for the as-synthesized $BaTiO_3$:Eu^{3+} powder at room temperature, and reveals the presence of $BaCO_3$ and TiO_2 starting materials which are observed until 700℃, as can be seen in this figure. In the following scans, between 600 and 1100℃, $BaTiO_3$ starts to crystallize on the basis of the appearance of the diffraction peak at 32°. The complete crystallization of $BaTiO_3$ powder occurs above 1100℃. On the other hand, the XRD patterns of $BaTiO_3$:Eu^{3+} powders heat-treated at 1150℃ were recorded at room temperature (Fig. 2). Figure 2(a) ascribed to the ssr sample reveals a fully crystallized $BaTiO_3$ with two diffraction peaks for (0 0 2) and (2 0 0) planes between 45 and 46°, as shown in the top inset. This splitting is characteristic of tetragonal $BaTiO_3$ [29].

To evaluate the phase transformation of the barium titanate at high temperatures, the sample after hydrothermal treatment was heat-treated from room temperature to 1200℃ in the HT-XRD chamber, and the different recorded XRD patterns are gathered in Fig. 1(b).

It can be noticed that the cubic structure formed after the hydrothermal treatment at 200℃ for 24 hours is stable up to 800℃. At higher temperatures from 800℃ to 1200℃, the patterns reveal a mixture of cubic and hexagonal $BaTiO_3$ in addition to $BaTi_2O_5$.

The phases present in $BaTiO_3$ powders after hydrothermal treatment were investigated by recording the XRD pattern at room temperature. Figure 2(b) shows well-crystallized $BaTiO_3$ with wider diffraction peaks in comparison with those obtained for ssr powders. Figure 2(b) also displays the magnified peak situated at $2\theta = 45°$; in this case, no splitting of the peak was observed, which is characteristic of a cubic perovskite structure of $BaTiO_3$. The mean size of crystallites (D) was calculated from the full-width at half maximum (FWHM) of the XRD peaks using Scherrer's equation [30]:

$$D = \frac{K\lambda}{\beta \cos\theta}$$

where λ (nm) represents the wavelength of the Cu Kα radiation (1.54056 Å), θ is Braggs's angle of the selected diffraction peak, β is the corrected half-width of the selected diffraction peak, and K is a geometric factor (K = 0.9 for spherical particles). Analyses of diffraction peaks for various samples showed that crystallite size is approximately 20 nm.

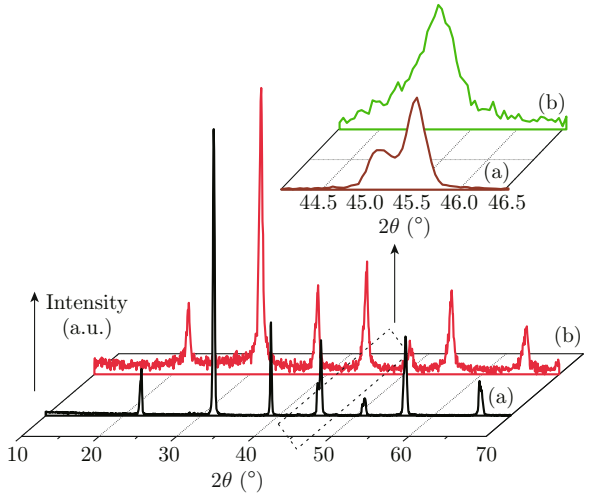

Fig. 2 XRD pattern of (a) ssr; (b) hm $BaTiO_3$:Eu^{3+} (5 mol%) powders recorded after respectively annealing for 4 h at 1150℃ and hydrothermal treatment for 24 h at 200℃.

Thermal analysis

In order to understand the synthesis process for $BaTiO_3$, TGA/DTA measurements were firstly performed for the ssr powders and exhibit decomposition in two steps (Fig. 3(a)). The first endothermic phenomenon appearing in the range of 20-450℃ is accompanied by a minimal loss of mass (3.5%) and can be attributed to the decomposition of $BaCO_3$. The next important event from 600 to 1000℃ reveals a larger loss of mass (12.8%) associated with an endothermic phenomenon, and can be ascribed to the following reaction: $BaCO_3+TiO_2 \rightarrow BaTiO_3+CO_2$. Figure 3(b) shows the TG curve of the hm sample, which reveals a total loss of mass (11.9%) in two steps, which is lower than that of the ssr powder (16.3%). The first loss (4.6%) below 200℃ was attributed to the release of adsorbed water and removing of remaining MeOH solvent. Between 200 and 800℃, the loss of mass can result from the decomposition of remaining alkoxy groups of butoxide precursor. Several defects, such as hydroxyl ions (OH^-), protons (H^+) or carbonates (CO_3^{2-}), are incorporated into the lattice during the hydrothermal process at high water pressure [31,32]. These defects stabilize the cubic phase, and hence decrease the tetragonality of the powder [33,34].

FT-IR characterization

The FT-IR spectrum of $BaTiO_3$ ssr powder is presented in Fig. 4(a). Two weak bands situated at 1430 cm^{-1} and 860 cm^{-1} are assigned to asymmetric stretching vibrations and out-of-plane bending vibrations of carboxylic groups respectively [35]. Besides, a weak

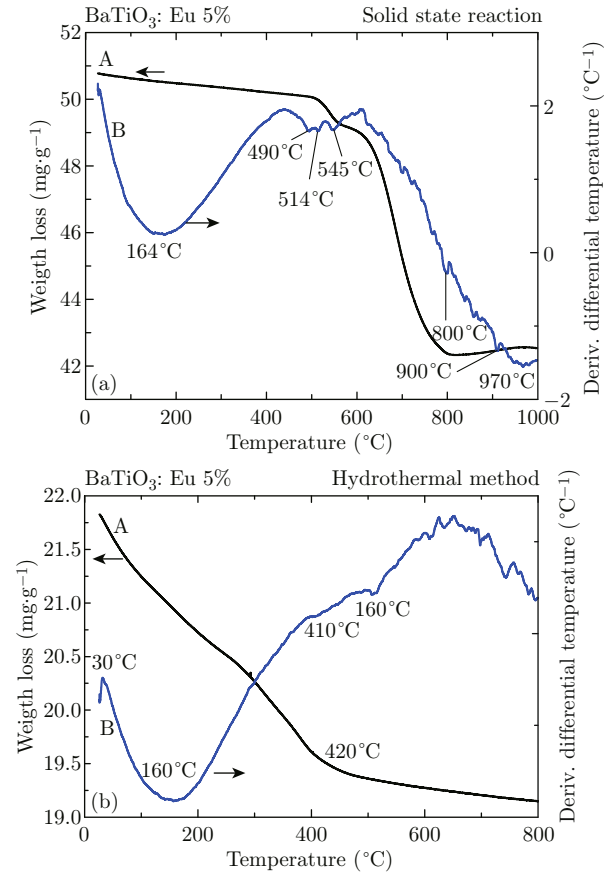

Fig. 3 DTA and TGA curves of (a) ssr; (b) hm $BaTiO_3$:Eu^{3+} (5 mol%) powders.

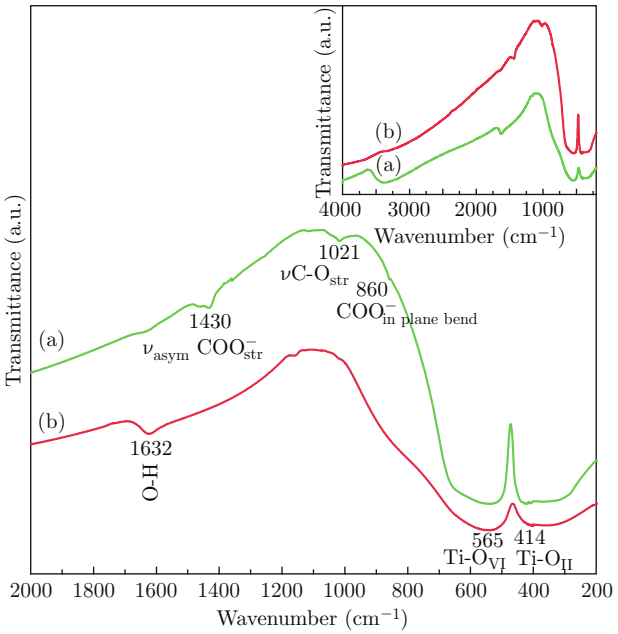

Fig. 4 IR spectra of (a) ssr; (b) hm $BaTiO_3$:Eu^{3+} (5 mol%) powders.

absorption band at about 1021 cm^{-1} is attributed to the alcoholic C-O stretching vibrations [36]. The broad band at around 414 cm^{-1} can be attributed to Ti-O_{II} bending normal vibrations [37], while the one situated at 565 cm^{-1} is assigned to the TiO_6 stretching vibrations connected to the barium [38]. Figure 4(b) shows the FT-IR spectrum of $BaTiO_3$ hm powder. This sample is characterized by a stretching band of hydroxyl (free and bonded) groups, respectively, in the range of 3600-3100 cm^{-1} and at 1632 cm^{-1} arising from bending vibrations of coordinated H_2O [39]. The two strong bands related to Ti-O bonds which are observed in the vicinity of 600-480 and 480–350 cm^{-1} are associated with Ti-O_I stretching vibrations to the vertical and the O_I-Ti-O_{II} bending vibrations [40] of a TiO_6 octahedron in the crystalline $BaTiO_3$ hm powder.

Raman Study

The Raman spectrum of ssr $BaTiO_3$ samples was collected at room temperature and is shown in Fig. 5(a). From this Fig. 5(a) the Raman fundamental modes (P4 mm) expected for tetragonal $BaTiO_3$ powders were observed [41,42]. According to Kaiser et al. [43] and Asiaie et al. [2], the weak shoulder below 300 cm^{-1} belongs to an A_1 (TO) phonon mode. The peak at ~307 cm^{-1} corresponds to an E(TO+LO) phonon mode of tetragonal $BaTiO_3$ [44], and the strong band peaking at ~515 cm^{-1} is attributed to an A_1 (TO) phonon mode of the tetragonal or cubic phase [45]. The weak peak at ~718 cm^{-1} has been associated with the highest-frequency longitudinal optical mode (LO) of A_1 symmetry. The Raman spectrum reported in Fig. 5(b) for hm $BaTiO_3$ powders reveals the same spectral features as the ssr $BaTiO_3$ sample with vibration modes at 718, 515, 306, and 260 cm^{-1}, which are also observed in the case of cubic structure. The only difference comes from the phonon mode A1(LO) at 185 cm^{-1}, which is unambiguously ascribed to the presence of the cubic $BaTiO_3$ phase.

SEM and TEM observations

Figure 6(a) shows the SEM micrograph recorded from ssr $BaTiO_3$:Eu^{3+} powder annealed for 4 h at

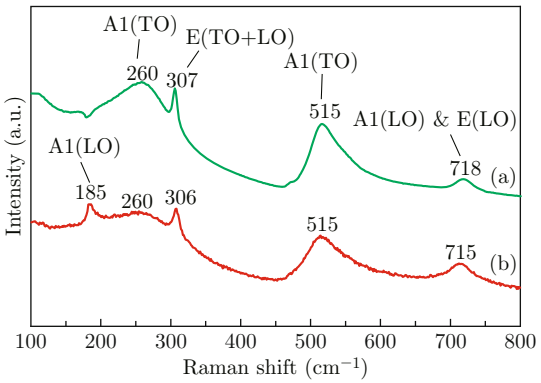

Fig. 5 Raman spectra of (a) ssr; (b) hm $BaTiO_3$:Eu^{3+} (5 mol%) powders.

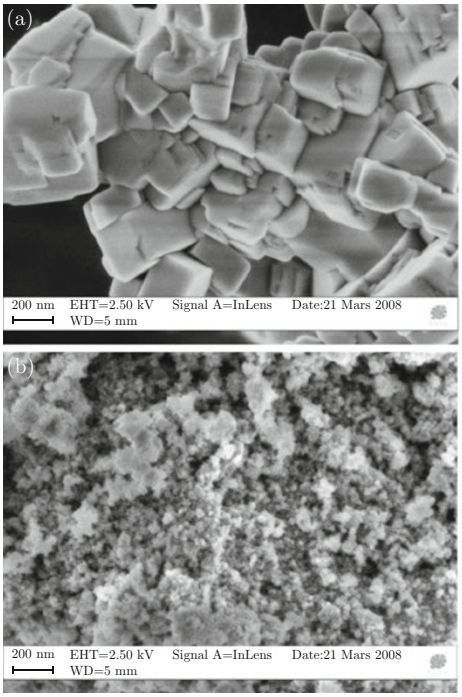

Fig. 6 SEM micrographs of (a) ssr; (b) hm $BaTiO_3$:Eu^{3+} (5 mol%) powders.

1150℃. The morphology consists of parallelogram-like particles exhibiting a noticeable agglomeration as well as a regular shape with an average length of about 200 nm.

The particle size and morphology of hm $BaTiO_3$:Eu^{3+} samples were firstly analyzed by SEM just after the product was washed and dried in an oven at 90℃ during 24 h. As shown in Fig. 6(b), the particle size is too low to be determined by this technique of electron microscopy. Thus, this sample was observed by TEM (Fig. 7(a)), and exhibited nanoparticles of a cubic shape. The average particle size distributions measured by image analyzer software (Fig. 7(b)) were statistically estimated to be 20 nm, as calculated from XRD patterns by the Scherrer formula.

Photoluminescence analysis

Figure 8 reports the $^7F_0 \rightarrow ^5D_2$ excitation spectra recorded at 300 K for the hm and ssr $BaTiO_3$:Eu^{3+} (5 mol%) samples by monitoring the overall $^5D_0 \rightarrow ^7F_2$ emission bands at 615.6 nm. Eu^{3+} ions are distributed in the Ba^{2+} site, i.e., one site of Oh symmetry and one site of C4v symmetry, respectively, in cubic and tetragonal phases. As a result, on the basis of the site symmetry, five and four Stark components are expected for the $^7F_0 \rightarrow ^5D_2$ transition, respectively, for the ssr and hm samples. This result is confirmed for ssr $BaTiO_3$:Eu^{3+} (5 mol%), whereas in the case of the hm sample, the $^7F_0 \rightarrow ^5D_2$ transition consists of a unique broad band which has been blue-shifted.

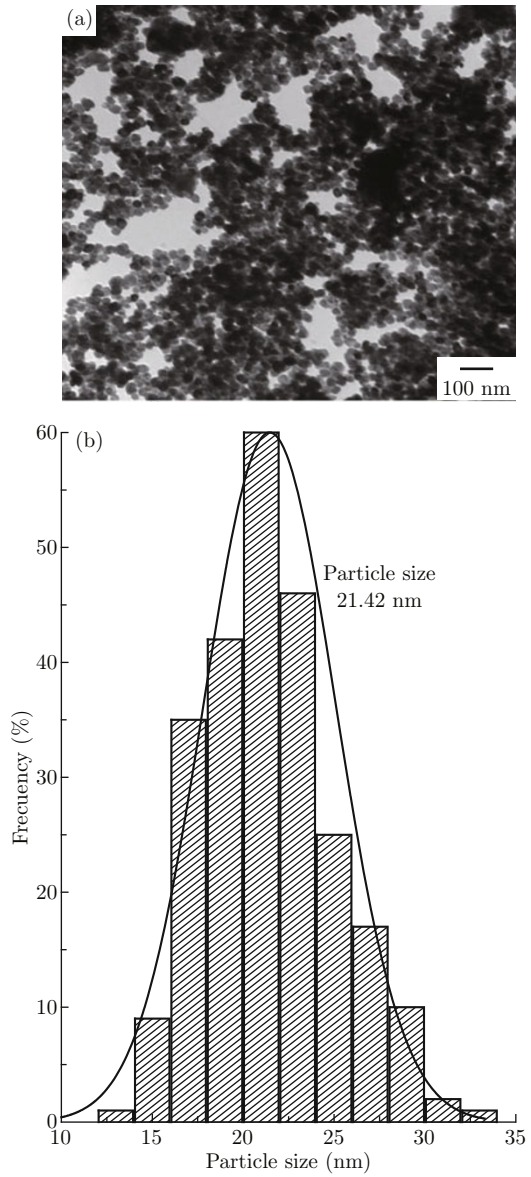

Fig. 7 TEM micrograph of (a) hm $BaTiO_3$:Eu^{3+} (5 mol%) powders; (b) particle size distribution.

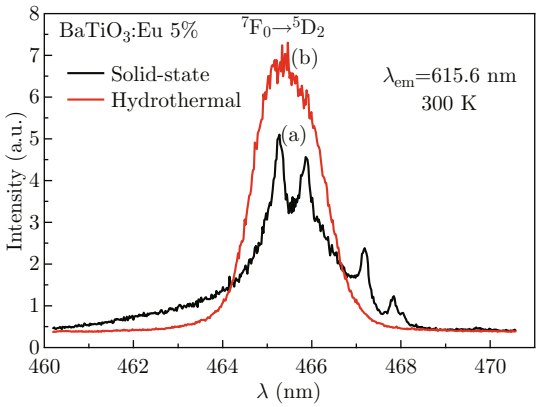

Fig. 8 $^7F_0 \rightarrow ^5D_2$ excitation spectra of (a) ssr; (b) hm (dashed line) $BaTiO_3$:Eu^{3+} (5 mol%) powders recorded at 300 K.

This peculiar spectral shape can be attributed to the embedding of Eu^{3+} ions in nano-size particles, which implies the same optical behavior as Eu^{3+} ions in amorphous powders [46]. Such an assumption is confirmed by the emission spectra recorded at 300 K upon excitation at 465.3 nm in the blue region (Fig. 9). Both spectra exhibit the typical $^5D_0 \rightarrow ^7F_{J=0-4}$ transitions of Eu^{3+} ions, but on the emission spectrum recorded from the ssr sample we can distinguish several Stark components for each transition, whereas this is not possible for the spectrum related to the hm sample.

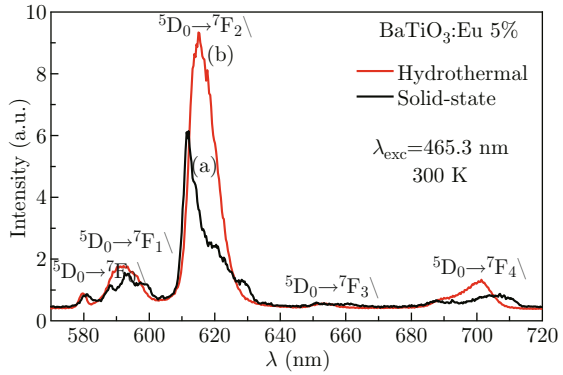

Fig. 9 Emission spectra of (a) ssr; (b) hm (dashed line) $BaTiO_3$:Eu^{3+} (5 mol%) powders recorded at 300 K upon excitation at 465.3 nm.

In this latter case, the spectrum is typical of Eu^{3+} ions embedded in an amorphous compound or in nanosized crystallites. As a result, each peak of $^5D_0 \rightarrow ^7F_{J=0-4}$ transitions is broadened and the intensity ratio $^5D_0 \rightarrow ^7F_2$ / $^5D_0 \rightarrow ^7F_1$ is dramatically increased, indicating a lowering of symmetry atanonlocal order.

Conclusion

$BaTiO_3$:Eu^{3+} (5 mol%) with a predominant cubic phase was successfully prepared by an original hydrothermal process using a titanium alkoxide as starting material. The formation of nanocrystallites was evidenced by XRD and MET analyses. Such a feature was confirmed by the photoluminescence investigation, which has demonstrated that the Eu^{3+} ions are embedded in nanosized powders in comparison with $BaTiO_3$:Eu^{3+} (5 mol%) samples prepared by the conventional solid-state reaction. Accordingly, the intensity of the $^5D_0 \rightarrow ^7F_2$ transition becomes much stronger than the one of the $^5D_0 \rightarrow ^7F_1$ transition, leading to a strong red fluorescence. Based on the theory of thermodynamic nucleation and growth, a short synthesizing process and low reaction temperature, compared with a solid-state reaction, reduce the possibility of particle growth. Besides, by using a hydrothermal method, it was possible to produce monosized distribution equiaxed $BaTiO_3$ powders with a predominant cubic phase of 20 nm, therefore facilitating the production of high-performance ceramic.

Acknowledgements

The authors gratefully acknowledge the financial support of the SEP-CONACYT (100764 & 178817) and SIP-IPN (20130664 and 20130665) projects. The authors also wish to acknowledge the financial support of this work by ECOSNord/ANUIES/CONACYT program number M09P01.

References

[1] H. Xu, L. Gao and J. Guo, "Hydrothermal synthesis of tetragonal barium titanate from barium chloride and titanium tetrachloride under moderate conditions", J. Am. Ceram. Soc. 85(3), 727-729 (2002). http://dx.doi.org/10.1111/j.1151-2916.2002.tb00163.x

[2] Mohammed A. Alam, Leonard Zuga and Michael G. Pecht, "Economics of rare earth elements in ceramic capacitors", Ceram. Inter. 38(8), 6091-6098 (2012). http://dx.doi.org/10.1016/j.ceramint.2012.05.068

[3] R. Pazik, D. Hreniak, W. Strek, V. G. Kessler and G. A. Seisenbaeva, "Photoluminescence investigations of Eu^{3+} doped $BaTiO_3$ nanopowders fabricated using heterometallic tetranuclear alkoxide complexes", J. Alloys Comp. 451(1-2), 557-562 (2008). http://dx.doi.org/10.1016/j.jallcom.2007.04.232

[4] J. Amami, D. Hreniak, Y. Guyot, R. Pazik, C. Goutaudier, G. Boulon, M. Ayadi and W. Strek, "Second harmonic generation and Yb^{3+} cooperative emission used as structural probes in size-driven cubic–tetragonal phase transition in $BaTiO_3$ sol-gel nanocrystals", J. Lumin. 119-120, 383-387 (2006). http://dx.doi.org/10.1016/j.jlumin.2006.01.021

[5] J. Amami, D. Hreniak, Y. Guyot, R. Pazik, W. Strek, C. Goutaudier and G. Boulon, "New optical tools used for characterization of phase transitions in nonlinear nano-crystals. Example of Yb^{3+}-doped $BaTiO_3$", J. Phys. Condens. Matter. 19(9), 1 (2007). http://dx.doi.org/10.1088/0953-8984/19/9/096204

[6] L. Chen, X. Wei and X. Fu, "Effect of Er substituting sites on upconversion luminescence of Er^{3+}-doped $BaTiO_3$ films", T. Nonferr. Metal. Soc. 22(5), 1156-1160 (2012). http://dx.doi.org/10.1016/S1003-6326(11)61299-5

[7] D. Hennings, G. Rosenstein and H. Schreinemacher, "Hydrothermal preparation of barium titanate from barium-titanium acetate gel precursors", J. Eur. Ceram. Soc. 8(2), 107-115 (1991). http://dx.doi.org/10.1016/0955-2219(91)90116-H

[8] T. Kimura, Q. Dong, S. Yin, T. Hashimoto and A. Sasaki, T. Sato. "Synthesis and piezoelectric properties of Li-doped $BaTiO_3$ by a solvothermal approach",

J. Eur. Ceram. Soc. 33(5), 1009-1015 (2013). http://dx.doi.org/10.1016/j.jeurceramsoc.2012.11.007

[9] W. W. Lee, W.-H. Chung, W-S. Huang, W.-C. Lin, W.-Y. Lin, Y.-R. Jiang and C.-C. Chen, "Photocatalytic activity and mechanism of nano-cubic barium titanate prepared by a hydrothermal method", J. Taiwan Inst. Chem. Eng. (2013). http://dx.doi.org/10.1016/j.jtice.2013.01.005

[10] X. Zhu, J. Zhu, S. Zhou, Z. Liu and N. Ming, "Photocatalytic activity and mechanism of nano-cubic barium titanate prepared by a hydrothermal method", J. Crystal Growth 310(2), 434-441 (2008). http://dx.doi.org/10.1016/j.jcrysgro.2007.10.076

[11] E. Ciftci, M. N. Rahaman and M. Shumsky, "Hydrothermal precipitation and characterization of nanocrystalline BaTiO3 particles", J. Mater. Sci. 36(20), 4875-4882 (2001). http://dx.doi.org/10.1023/A:1011828018247

[12] J. Yuh, L. Perez, W. M. Sigmund and J. C. Nino, "Sol-gel based synthesis of complex oxide nanofibers", J. Sol-Gel Sci. Technol. 42(3), 323-329 (2007). http://dx.doi.org/10.1007/s10971-007-0736-6

[13] Z. Xinle, M. Zhimei, X. Zuojiang and C. Guang, "Preparation and characterization on nano-sized barium titanate powder doped with lanthanum by sol-gel process", J. Rare Earths 24(1), 82-85 (2006). http://dx.doi.org/10.1016/S1002-0721(07)60329-9

[14] M. Cernea, O. Monnereau, P. Llewellyn, L. Tortet and Carmen Galassi, "Sol-gel synthesis and characterization of Ce doped-$BaTiO_3$", J. Eur. Ceram. Soc. 26(15), 3241-3246 (2006). http://dx.doi.org/10.1016/j.jeurceramsoc.2005.09.039

[15] D. Hreniak, W. Strek, J. Chmielowiec, G. Pasciak, R. Pazik, S. Gierlotka and W. Lojkowski, "Preparation and conductivity measurement of Eu doped $BaTiO_3$ nanoceramic", J. Alloys Comp. 408-412, 637-640 (2006). http://dx.doi.org/10.1016/j.jallcom.2004.12.098

[16] M. A. Meneses-Nava, O. Barbosa-García, J. L. Maldonado, G. Ramos-Ortíz, J. L. Pichardo, M. Torres-Cisneros, M. García-Hernández, A. García-Murillo and F. J. Carrillo-Romo, "Yb^{3+} quenching effects in co-doped polycrystalline $BaTiO_3$:Er^{3+}, Yb^{3+}", Opt. Mater. 31(2), 252-260 (2008). http://dx.doi.org/10.1016/j.optmat.2008.04.002

[17] L. Simon-Seveyrat, A. Hajjaji, Y. Emziane, B. Guiffard and D. Guyomar, "Re-investigation of synthesis of $BaTiO_3$ by conventional solid-state reaction and oxalate coprecipitation route for piezoelectric applications", Ceram. Inter. 33(1), 35-40 (2007). http://dx.doi.org/10.1016/j.ceramint.2005.07.019

[18] Y. Sakabe, Y. Yamashita and H. Yamamoto, "Dielectric properties of nano-crystalline $BaTiO_3$ synthesized by micro-emulsion method", J. Eur. Ceram. Soc. 25(12), 2739-2742 (2005). http://dx.doi.org/10.1016/j.jeurceramsoc.2005.03.226

[19] K. H. Felner, T. Muller, H. T. Langhammer and H. P. Abicht, "On the formation of $BaTiO_3$ from $BaCO_3$ and TiO_2 by microwave and conventional heating", Mater. Lett. 58(12-13), 1943-1947 (2004). http://dx.doi.org/10.1016/j.matlet.2003.11.037

[20] V. Vinothini, P. Singh and M. Balasubramanian, "Synthesis of barium titanate nanopowder using polymeric precursor method", Ceram. Inter. 32(2), 99-103 (2006). http://dx.doi.org/10.1016/j.ceramint.2004.12.012

[21] Z. C. Hu, G. A. Miller, E. A. Payzant and C. J. Rawn, "Homogeneous (co)precipitation of inorganic salts for synthesis of monodispersed barium titanate particles", J. Mater. Sci. 35(12), 2927-2936 (2000). http://dx.doi.org/10.1023/A:1004718508280

[22] M. Yoshimura and K. Byrappa, "Hydrothermal processing of materials: past, present and future", J. Mater. Sci. 43(7), 2085-2103 (2008). http://dx.doi.org/10.1007/s10853-007-1853-x

[23] D. E. Rase and R. Roy, "Phase equilibria in the system BaO-TiO_2", J. Am. Ceram. Soc. 38(3), 102–113. (1955). http://dx.doi.org/10.1111/j.1151-2916.1955.tb14585.x

[24] J.-H. Kim, W.-S. Jung, H.-T. Kim and D.-H. Yoon, "Properties of $BaTiO_3$ synthesized from barium titanyl oxalate", Ceram. Inter. 35(6), 2337-2342 (2009). http://dx.doi.org/10.1016/j.ceramint.2009.01.006

[25] K. Ishikawa, K. Yoshikawa and N. Okada, "Size effect on the ferroelectric phase transition in $PbTiO_3$ ultrafine particles", Phys. Rev. B 37(10), 5852-5855 (1988). http://dx.doi.org/10.1103/PhysRevB.37.5852

[26] S. Schlag and H. F. Eicke, "Size driven phase transition in nanocrystalline $BaTiO_3$", Solid State Commun. 91(11), 883-887 (1994). http://dx.doi.org/10.1016/0038-1098(94)90007-8

[27] M. K. Rath, G. K. Prahdan, B. Pandey, H. C. Verma, B. K. Roul and S. Anand, "Synthesis, characterization and dielectric properties of europium-doped barium titanate nanopowders", Mater. Lett. 62(14), 2136-2139 (2008). http://dx.doi.org/10.1016/j.matlet.2007.11.033

[28] R. Pazik, R. J. Wiglusz and W. Strek, "Luminescence properties of $BaTiO_3$:Eu^{3+} obtained via microwave stimulated hydrothermal method", Mater. Res. Bull. 44(6), 1328-1333 (2009). http://dx.doi.org/10.1016/j.materresbull.2008.12.010

[29] S. Zhang, F. Jiang, Gang Qu and C. Lin, "Synthesis of single-crystalline perovskite barium titanate nanorods by a combined route based on sol-gel and surfactant-templated methods", Mater. Lett. 62(15), 2225-2228 (2008). http://dx.doi.org/10.1016/j.matlet.2007.11.055

[30] A. L. Patterson, "The scherrer formula for X-ray particle size determination", Phys. Rev. 56(10), 978-982 (1939). http://dx.doi.org/10.1103/PhysRev.56.978

[31] F. K. Detlev Hennings, C. Metzmacher and B. Seriyati Schreinemacher, "Defect chemistry and microstructure of hydrothermal barium titanate", J. Am. Ceram. Soc. 84(1), 179-182 (2001). http://dx.doi.org/10.1111/j.1151-2916.2001.tb00627.x

[32] S.-W. Kwon and D.-H. Yoon. "Tetragonality of nano-sized barium titanate powder prepared with growth inhibitors upon heat treatment", J. Eur. Ceram. Soc. 27(1), 247-252 (2007). http://dx.doi.org/10.1016/j.jeurceramsoc.2006.02.031

[33] G. Arlt, D. Hennings and G. de With, "Dielectric properties of fine-grained barium titanate ceramics", J. Appl. Phys. 58(4), 1619-1625 (1985). http://dx.doi.org/10.1063/1.336051

[34] J. Nowotny and M. Rekas, "Defect chemistry of $BaTiO_3$", Solid State Ionics 49, 135-154 (1991). http://dx.doi.org/10.1016/0167-2738(91)90079-Q

[35] L. Li, Y. Chu, Y. Liu, L. Dong, L. Huo and F. Yang, "Microemulsion-based synthesis of $BaCO_3$ nanobelts and nanorods", Mater. Lett. 60(17-18), 2138-2142 (2006). http://dx.doi.org/10.1016/j.matlet.2005.12.087

[36] P. Yu, B. Cui and Q. Shi. "Preparation and characterization of $BaTiO_3$ powders and ceramics by sol-gel process using oleic acid as surfactant", Mater. Sci. Eng. A 473(1-2), 34-41 (2008). http://dx.doi.org/10.1016/j.msea.2007.03.051

[37] S. Ghosh, S. Dasgupta, A. Sen and H. S. Maiti. "Synthesis of barium titanate nanopowder by a soft chemical process", Mater. Lett. 61(2), 538-541 (2007). http://dx.doi.org/10.1016/j.matlet.2006.05.006

[38] A. García Murillo, F. J. Carrillo Romo, M. García Hernández, J. Ramírez Salgado, M. A. Domínguez Crespo, S. A. Palomares Sánchez and H. Terrones, "Structural and morphological characteristics of polycrystalline $BaTiO_3$:Er^{3+}, Yb^{3+} ceramics synthesized by the sol-gel route: influence of chelating agents", J Sol-Gel Sci. Technol. 53(1), 121 (2010). http://dx.doi.org/10.1007/s10971-009-2069-0

[39] Y. Gao, Y. Masuda, Z. Peng, T. Yonezawa and K. Koumoto, "Room temperature deposition of a TiO_2 thin film from aqueous peroxotitanate solution", J. Mater. Chem. 13, 608-613 (2003). http://dx.doi.org/10.1039/b208681f

[40] K. Sadhana, T. Krishnaveni, K. Praveena, S. Bharadwaj and S. R. Murthy, "Microwave sintering of nano-barium titanate", Scripta Materialia 59(5), 495-498 (2008). http://dx.doi.org/10.1016/j.scriptamat.2008.04.036

[41] R. Cho, S. H. Kwun, T. W. Noh and M. S. Jang, "Electrical properties of sol-gel deposited $BaTiO_3$ thin films on Si(100) substrates", Jpn. J. Appl. Phys. 36, 2196-2199 (1997). http://dx.doi.org/10.1143/JJAP.36.2196

[42] W. K. Kuo and Y. C. Ling, "Effects of mono-substituting chelating agents on $BaTiO_3$ prepared by the sol-gel process", J. Mater. Sci. 29(21), 5625-5630 (1994). http://dx.doi.org/10.1007/BF00349957

[43] L. Kaiser, M. D. Vaudin, G. Gillen, C. S. Hwang, L. H. Robins and L. D. Rotter, "Growth and characterization of barium titanate thin films prepared by metalorganic chemical vapor deposition", J. Crystal Growth 137(1-2), 136-140 (1994). http://dx.doi.org/10.1016/0022-0248(94)91261-0

[44] C. J. Xiao, C. Q. Jin and X. H. Wang, "Crystal structure of dense nanocrystalline $BaTiO_3$ ceramics", Mater. Chem. Phys., 111(2-3), 209-212 (2008). http://dx.doi.org/10.1016/j.matchemphys.2008.01.020

[45] H. X. Zhang, C. H. Kam, Y. Zhou, X. Q. Han, Y. L. Lam, Y. C. Chan and K. Pita, "Optical and electrical properties of sol-gel derived $BaTiO_3$ films on ITO coated glass", Mater. Chem. Phys., 63(2), 174-177 (2000). http://dx.doi.org/10.1016/S0254-0584(99)00222-9

[46] C. H. Yan, L. D. Sun, C. S. Liao, Y. X. Zhang, Y. Q. Lu, S. H. Huang and S. Z. Lü, "Eu^{3+} ion as fluorescent probe for detecting the surface effect in nanocrystals", Appl. Phys. Lett. 82(20), 3511-3513 (2003). http://dx.doi.org/10.1063/1.1575504